Supplementary Figures

Fast, robust and precise 3D localization for arbitrary point spread functions

Yiming Li[1], Markus Mund[1], Philipp Hoess[1], Ulf Matti[1], Bianca Nijmeijer[1], Vilma Jimenez Sabinina[1], Jan Ellenberg[1], Ingmar Schoen[2] & Jonas Ries[1*]

[1]European Molecular Biology Laboratory (EMBL), Cell Biology and Biophysics unit, Meyerhofstr. 1, 69117 Heidelberg, Germany
[2]Royal College of Surgeons in Ireland, 123 St. Stephen's Green, Dublin 2, Ireland

[*]Correspondence should be addressed to J.R. (jonas.ries@embl.de)

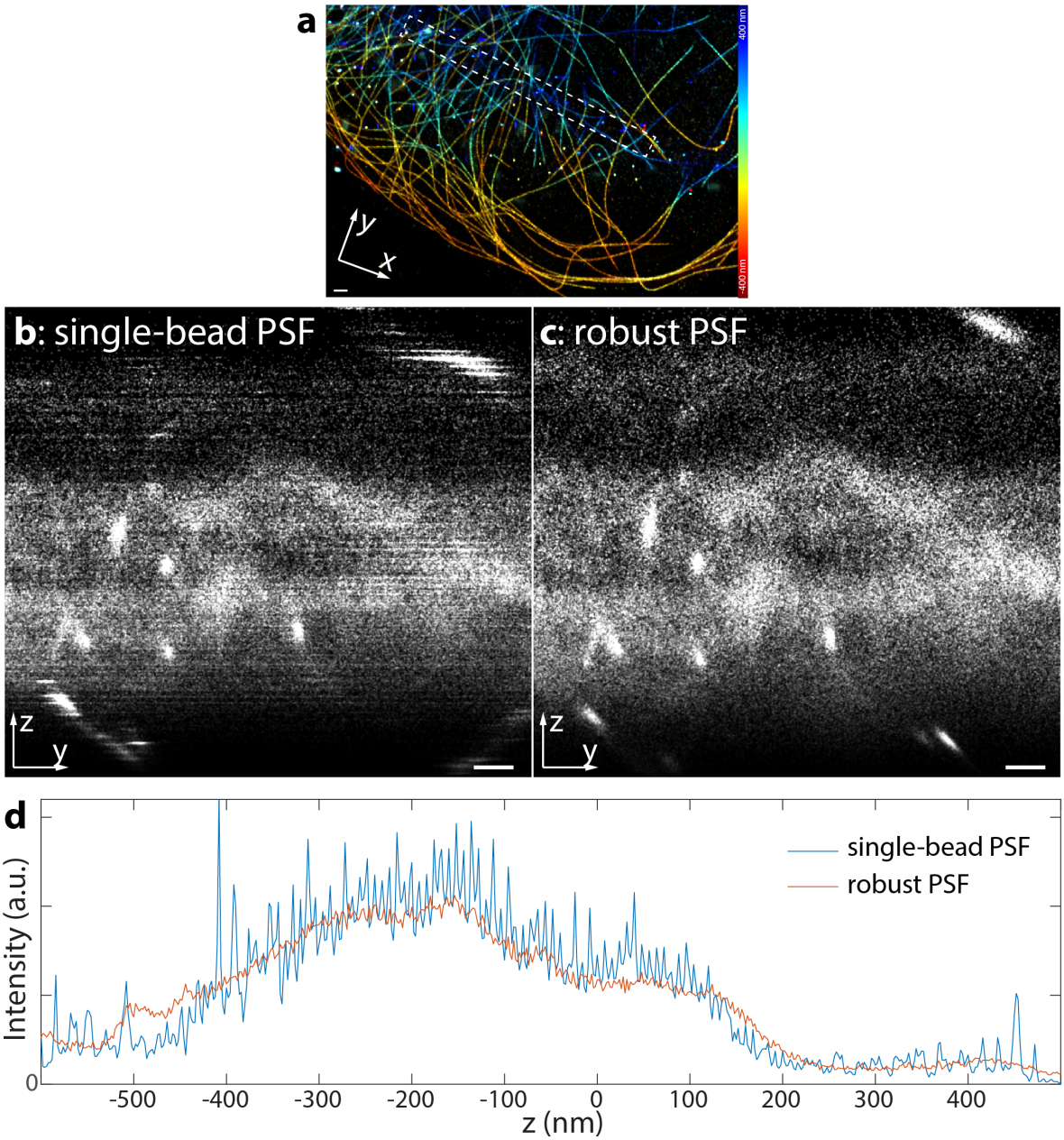

Supplementary Figure 1: Noisy PSF model leads to stripe artifacts

(**a**) Overview image of microtubules in a U-2 OS cell. The axial positions were color coded according to the color scale bar. (**b**) *y*-*z* plot of the boxed region in (**a**) when the PSF was modeled using only a single bead without smoothing. (**c**) *y*-*z* plot of the boxed region in (**a**) when PSF was robustly modeled with many beads across different fields of view and with regularization, as described in **Online Methods**. (**d**) *z*-profiles of (**b**) and (**c**). The stripe artifact is avoided using the proper averaging and regularization. Scale bars: (**a**) 1 µm, (**b**), (**c**) 100 nm.

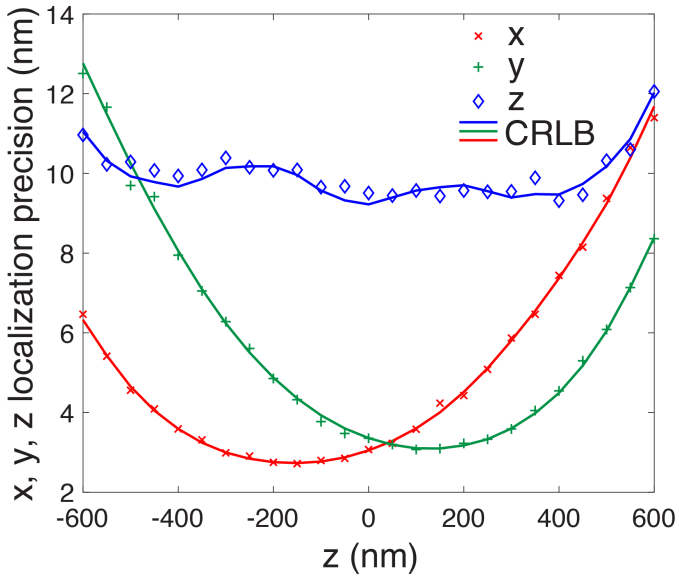

Supplementary Figure 2: The localization precision of the fitter achieves minimum uncertainty on the cspline interpolated experimental astigmatic PSF

Single molecule images were simulated using an experimental astigmatic PSF model with 5000 photons/localization and 10 background photons/pixel and fitted with the interpolated cubic spline model. We then evaluated the *x*, *y* and *z* localization precisions at different axial positions as the standard deviation of the error between fitted 3D positions and ground truth of the 10000 simulated molecules at each axial position. The localization precision of the fitted positions achieves the estimated CRLB (denoted by lines) in all 3 dimensions.

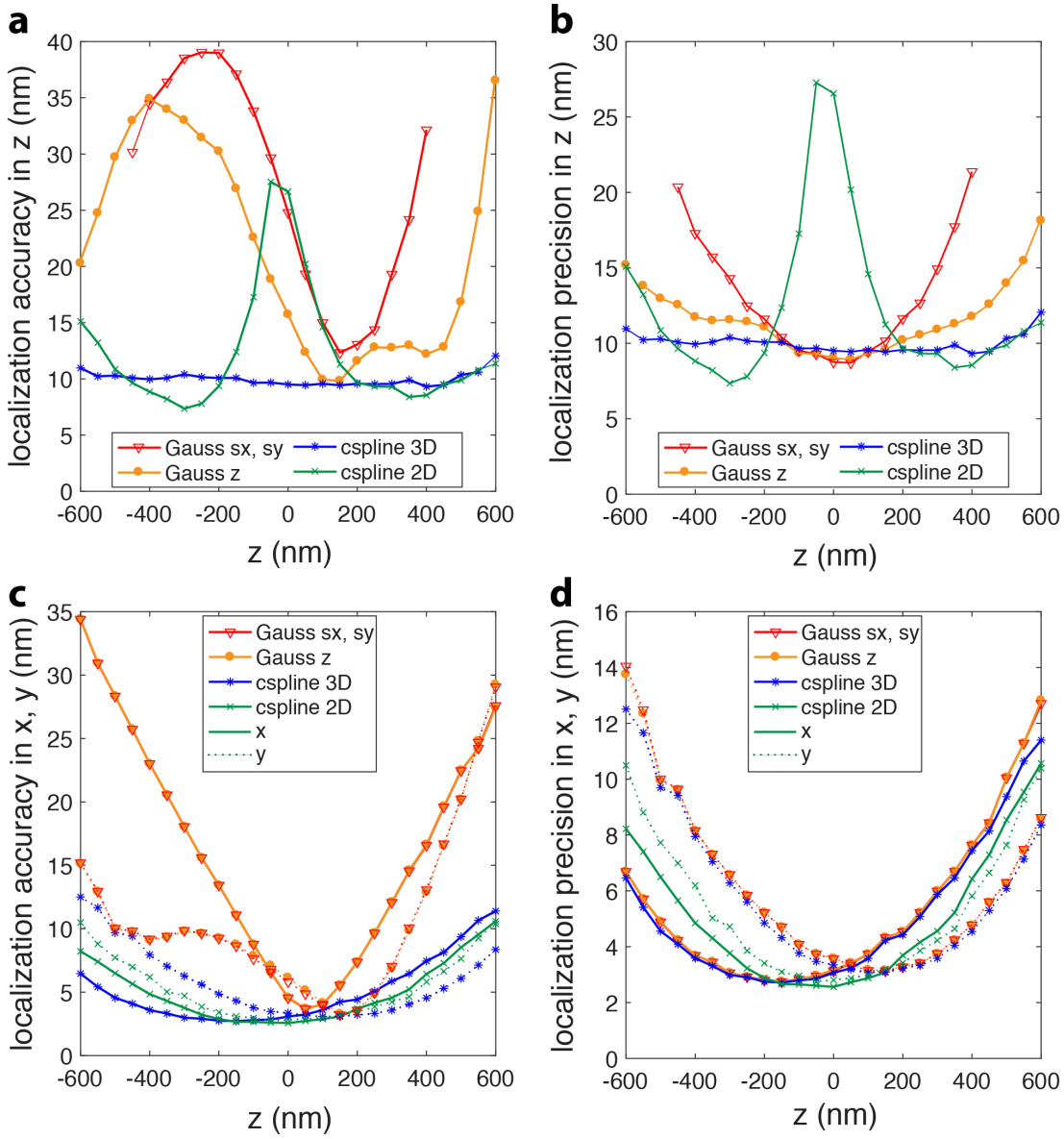

Supplementary Figure 3: Localization precision and accuracy of Gaussian versus experimental PSF model

Single molecule images were simulated using an experimental PSF model with 5000 photons/localization and 10 background photons/pixel. For the cspline 3D and elliptical Gaussian fit, an experimental astigmatic PSF was used for the simulation. For the cspline 2D fit, an unmodified experimental PSF was used. We then evaluated both localization precision and accuracy in 3D at different axial positions from 1000 simulated molecules at each axial position. The *localization precision* is calculated as the *standard deviation* of the difference between the fitted positions and ground truth positions, and the *localization accuracy* is calculated as the *root mean square error* between the fitted positions and ground truth positions. (**a**) Localization accuracy and (**b**) localization precision in *z* for different models at different axial positions. For the elliptical Gaussian PSF model, two algorithms were used for *z* localization as described in **Online Methods**. (**c**, **d**) are the same as (**a**, **b**) but in lateral direction, respectively.

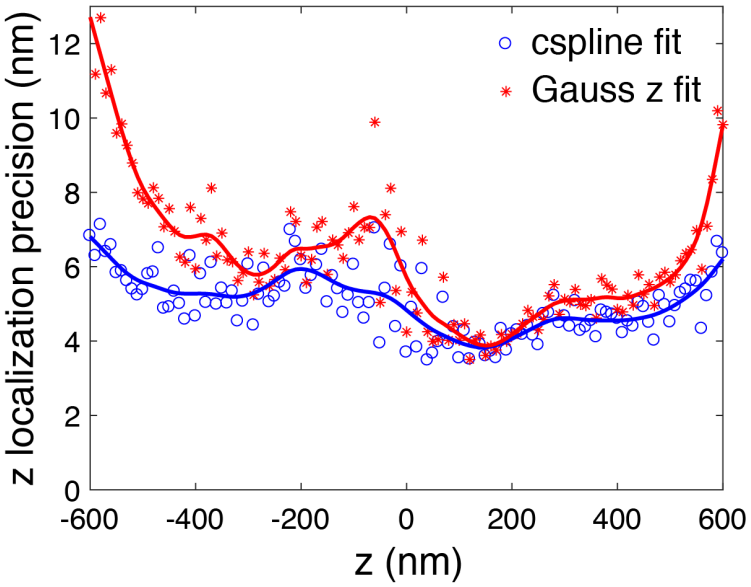

Supplementary Figure 4: Experimental axial localization precision for Gaussian and cspline interpolated experimental PSF model

A fluorescent bead was attached on cover glass and imaged axially by translating the piezo stage. 100 frames were acquired at each 10 nm step. The bead was fitted with the Gaussian PSF and the cspline interpolated PSF model, respectively. The localization precision in *z* was determined as the standard deviation of the returned positions at each step (100 positions). The localization precision of the cspline fit is better than the Gaussian fit in most cases. Especially in the regions far away from the focus, the performance is typically improved by about 30~50%. The solid lines are smoothing interpolations.

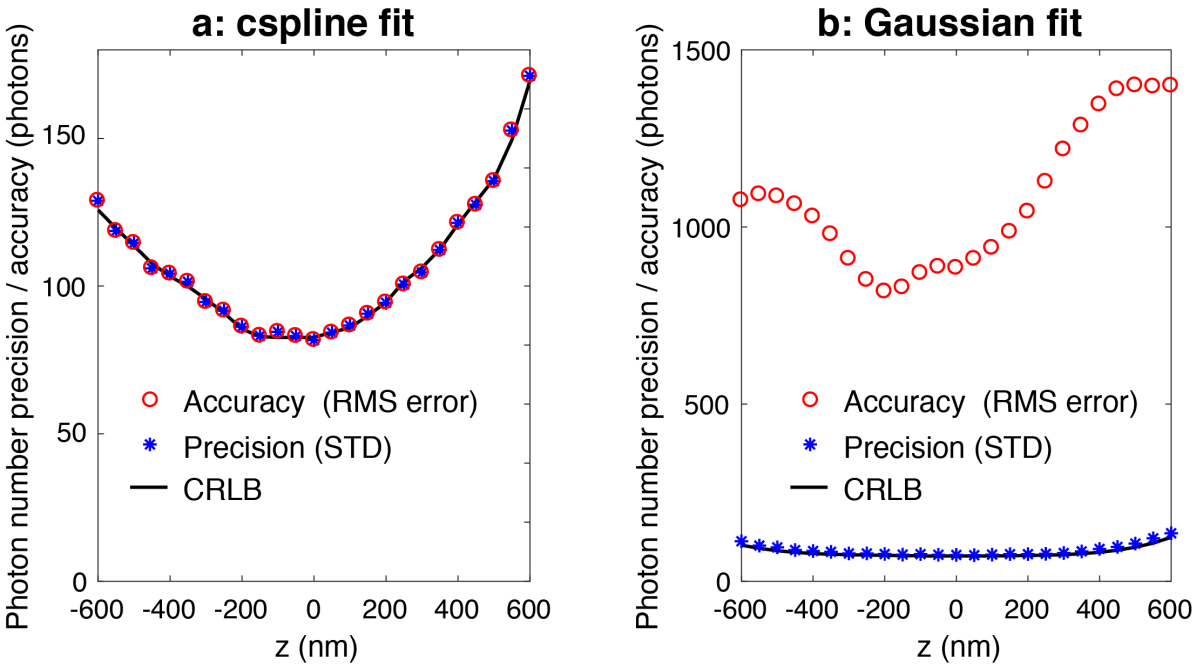

Supplementary Figure 5: Precision and accuracy in determining photon numbers
Single molecule images were simulated using an experimental astigmatic PSF model with 5000 photons/localization and 10 background photons/pixel. Accuracy (root mean square error) and precision (standard deviation) of fitted photons/localization at different axial positions for (**a**) cspline fit and (**b**) Gaussian fit. The Gaussian fit has a strong systematic error in estimating the photons/localization.

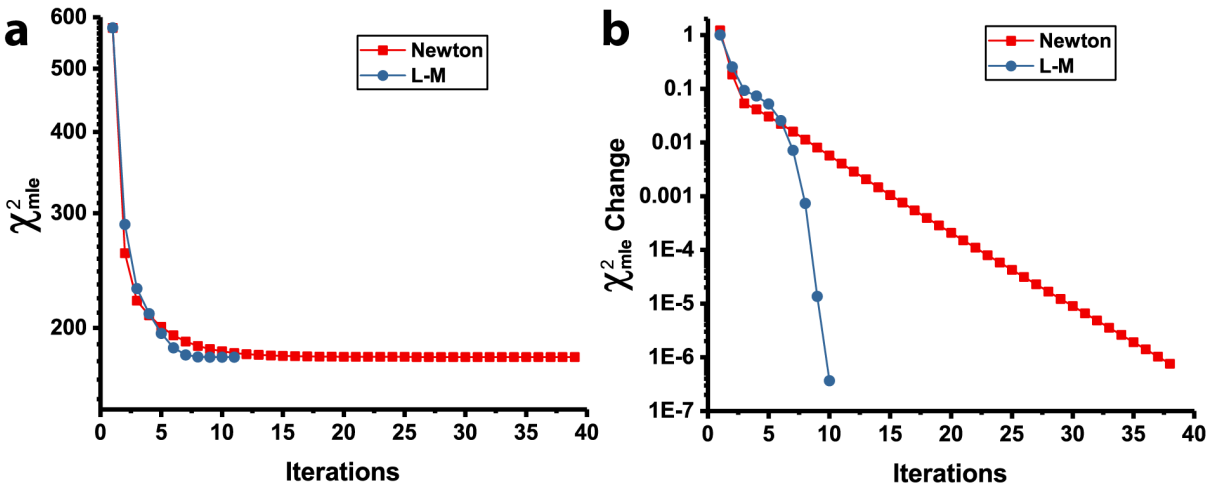

Supplementary Figure 6: Convergence of Levenberg-Marquardt and Newton iterative method

We compared for the L-M and Newton method (elliptical Gaussian PSF model) the change of the MLE cost function χ^2_{mle} at each iteration. χ^2_{mle} is defined as in ref. 1 (main manuscript), $\chi^2_{\text{mle}} = 2(\sum_k(\mu_k - x_k) - \sum_{k,x_k>0} x_k \ln(\mu_k/x_k))$, where, μ_k are the expected photons in pixel k from the model function, x_k are the measured photons. By minimizing χ^2_{mle}, we obtain the maximum likelihood for the Poisson process. Here we compared the Newton iterative scheme for the minimization used in the previous published GPU Gaussian fitting with the L-M algorithm as used in this work. The test data were simulated with an elliptical Gaussian model with sigma 1.5 and 2.5 pixels in x and y, respectively. We used 500 photons per localization and 10 background photons per pixel. The iteration stops when the relative change of χ^2_{mle} decreases by less than 1E-6. The number of iterations is 39±6 for the Newton method and 11±1 for the L-M method, which indicates the L-M method is more efficient than the custom Newton solver. (**a**) Update of χ^2_{mle} during each iteration. (**b**) Relative change of χ^2_{mle} during each iteration. The Newton method converges faster in the first few iterations. However, it becomes slow in the later steps.

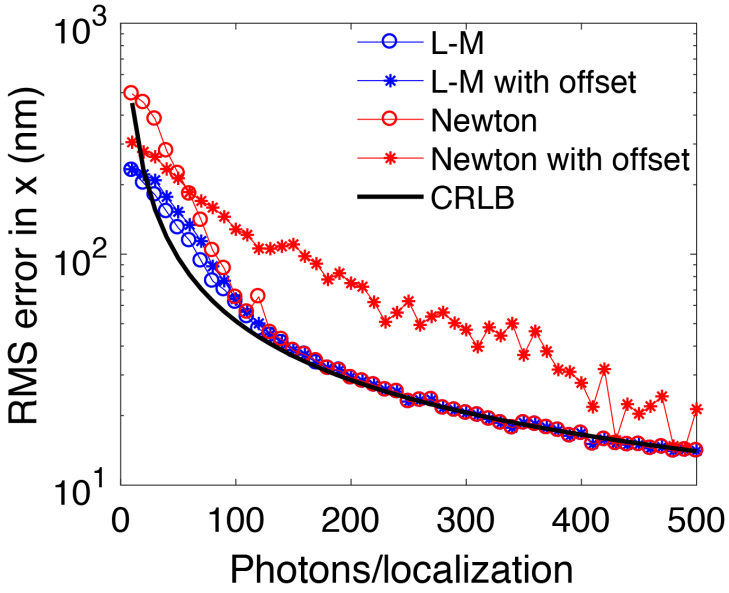

Supplementary Figure 7. The Levenberg-Marquardt algorithm is more robust with respect to starting parameters than the Newton method

An elliptical Gaussian model with $\sigma_x = 1.5$ pixels and $\sigma_y = 2.5$ pixels was used for data simulation. The background is fixed at 5 photons per pixel. The localization precision from a fit with a Gaussian PSF model is plotted as a function of photons/localization. For estimating the localization precision, 1000 single molecules with box sizes of 13 ×13 were generated at each data point. The maximum number of iterations was 100. Both these two algorithms could achieve the theoretical CRLB for molecules with more than 100 photons. The centroid of the fitting window was used as intimal parameters in both fitting routines. As the single molecule fitting window is often contaminated by nearby molecules or background signals, the centroid of the fitting window is often offset by more than one pixel compared to the position of the fluorophore. We thus purposely offset the initial x, y coordinates (centroid) by 2 pixels and investigated how this affects the localization precision. Whereas the final localization precision for the L-M algorithm is robust with respect to the start parameters, the Newton method often fails to converge for a wrong starting parameter estimate.

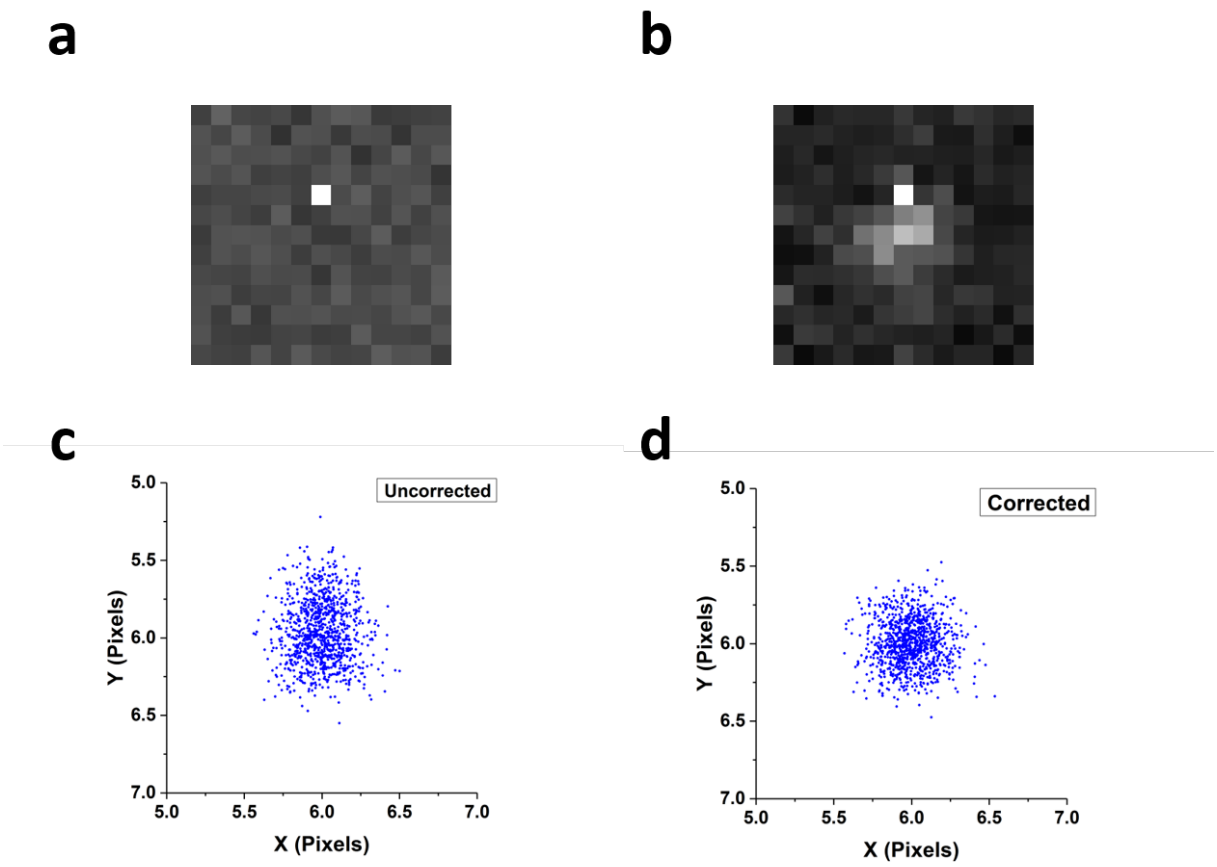

Supplementary Figure 8: sCMOS noise model avoids readout noise induced bias
Single-molecule images were simulated considering pixel-dependent readout noise, as is present in sCMOS cameras. The readout noise of the overall pixels is set as a Gaussian distribution with a mean of 1.4 e^- and a sigma with 0.2 e^-. (**a**) The map of the readout noise. The readout noise of the pixel located 2 pixels to the up of the center is set as 30 e^-. (**b**) Simulated single molecule with the readout noise as shown in (**a**). Each molecule was simulated as 2D Gaussian with a width of $\sigma = 1.4$ pixels, 200 photons/localization and 2 background photons/pixel. The positions of the molecules were all placed in the center (6, 6) of the window. (**c**) Scatter plot of the 1,000 fitted positions of the molecules as shown in (**b**) fitted with the EMCCD noise model. (**d**) Scatter plot of the 1000 fitted positions of the molecules as shown in (**b**) fitted with the sCMOS noise model.

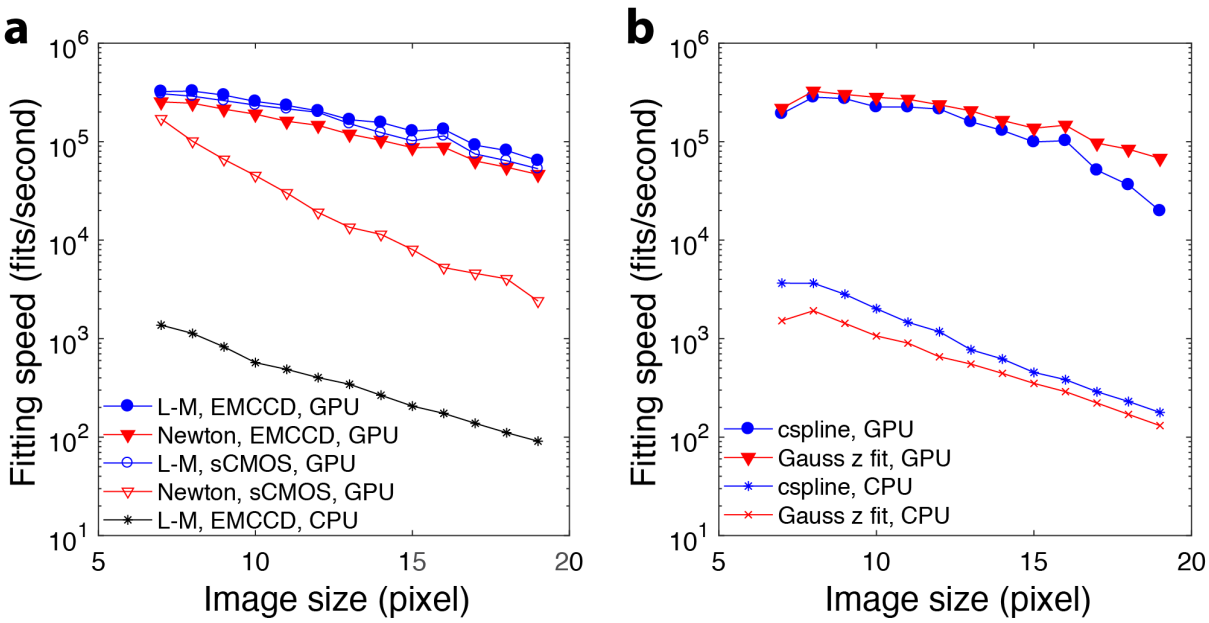

Supplementary Figure 9: Computational speed of different fitting routines
(**a**) Comparison of the speed of the Newton method and the L-M algorithm using an elliptical Gaussian PSF model. The effect of the readout noise variance for sCMOS camera data was also evaluated. Even though the L-M algorithm has higher complexity as it evaluates χ^2_{mle} every iteration to determine the damping factor, it is still slightly faster than Newton method due to the fact that less iterations are needed. (**b**) Comparison of the speed of astigmatic Gauss *z* fit and cspline *z* fit. The GPU code is overall more than 100 times faster than the CPU code running on a single thread. It is interesting to notice that the spline fit is even faster than the Gauss z fit in the CPU code while it is slower than the Gauss z fit in GPU code. This is probably because the spline coefficients are accessed much more frequently in the GPU than the CPU, which slows down the performance.

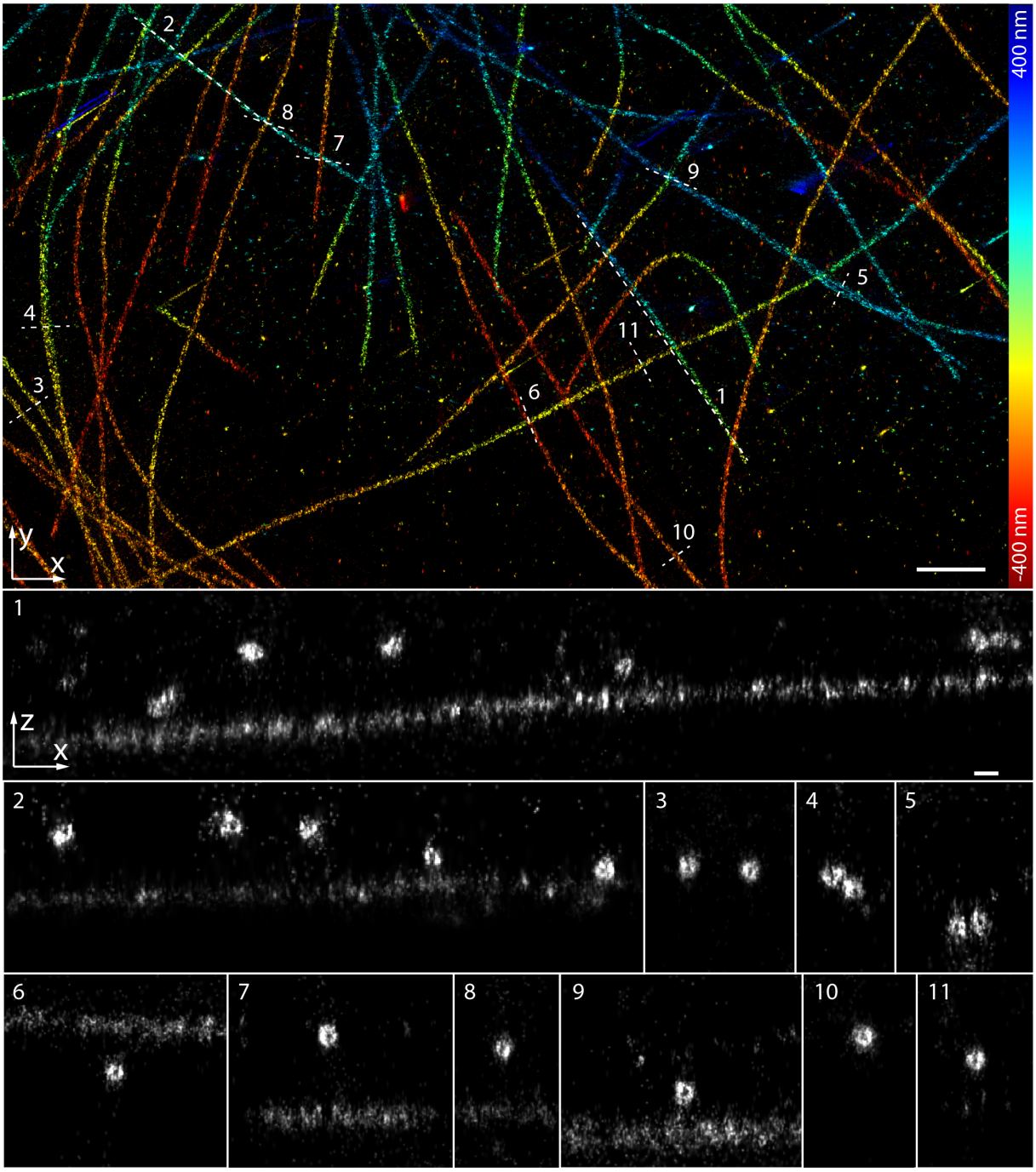

Supplementary Figure 10: 3D astigmatic dSTORM image of microtubules

Microtubules in U-2 OS cells, labeled with primary alpha-tubulin antibodies and secondary Alexa Fluor 647 antibodies were imaged with a cylindrical lens. Upper panel: *x*-*y* top view. Lines denote regions for which *x*-*z* (side view) cross-sections are shown in the lower panels. The width of the regions used to calculate the cross-sections was 250 nm. Corresponding localization precisions and profiles can be found in **Supplementary Fig. 11.** Scale bars: 1 µm (top view), 100 nm (side views).

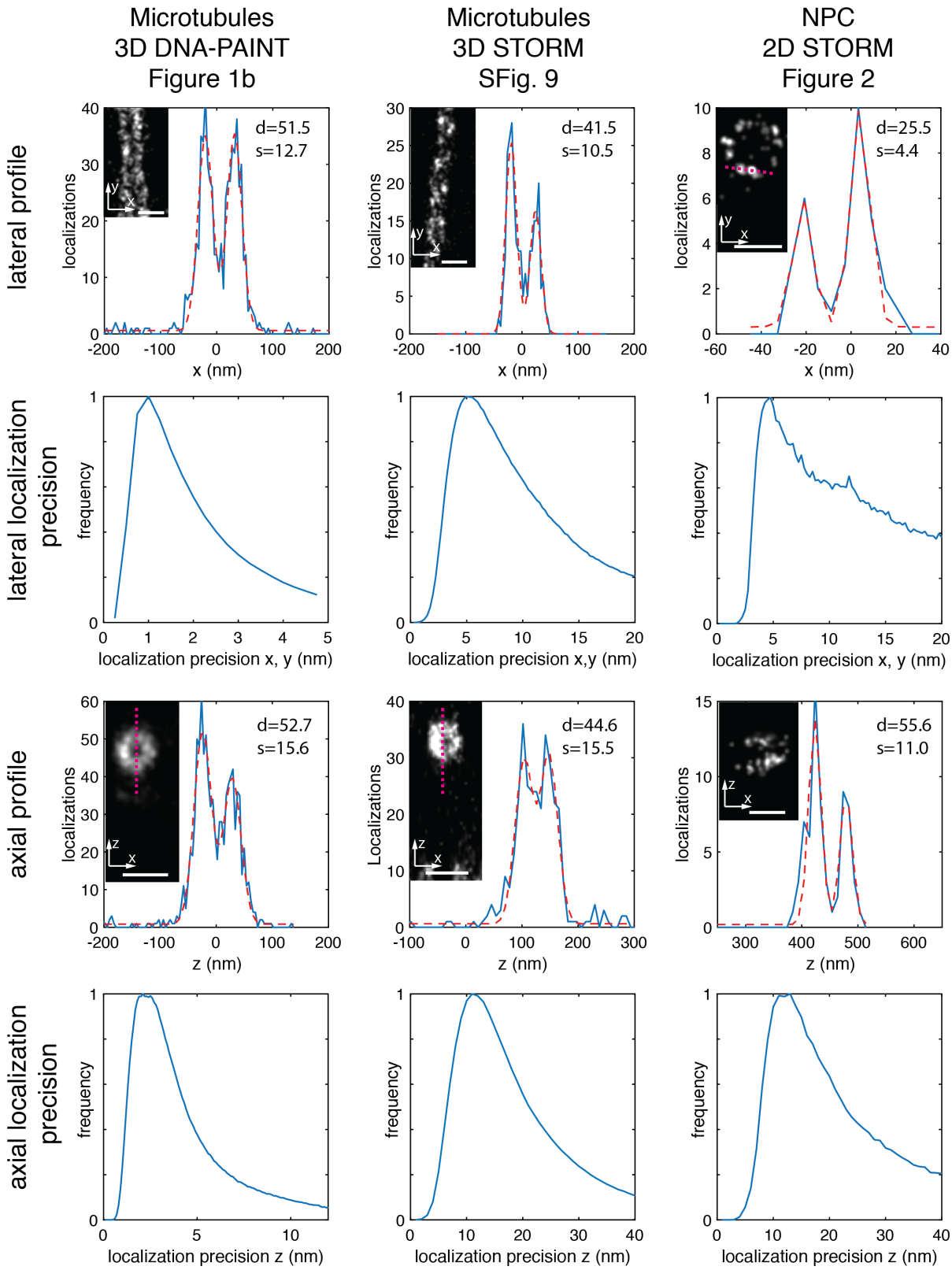

Supplementary Figure 11: Experimental profiles and localization precisions for the data used in this manuscript. The insets denote the regions where the profiles were taken. Dotted lines: Fit with two Gaussians with a distance *d* and a standard deviation *s* in nm. Scale bars 100 nm.

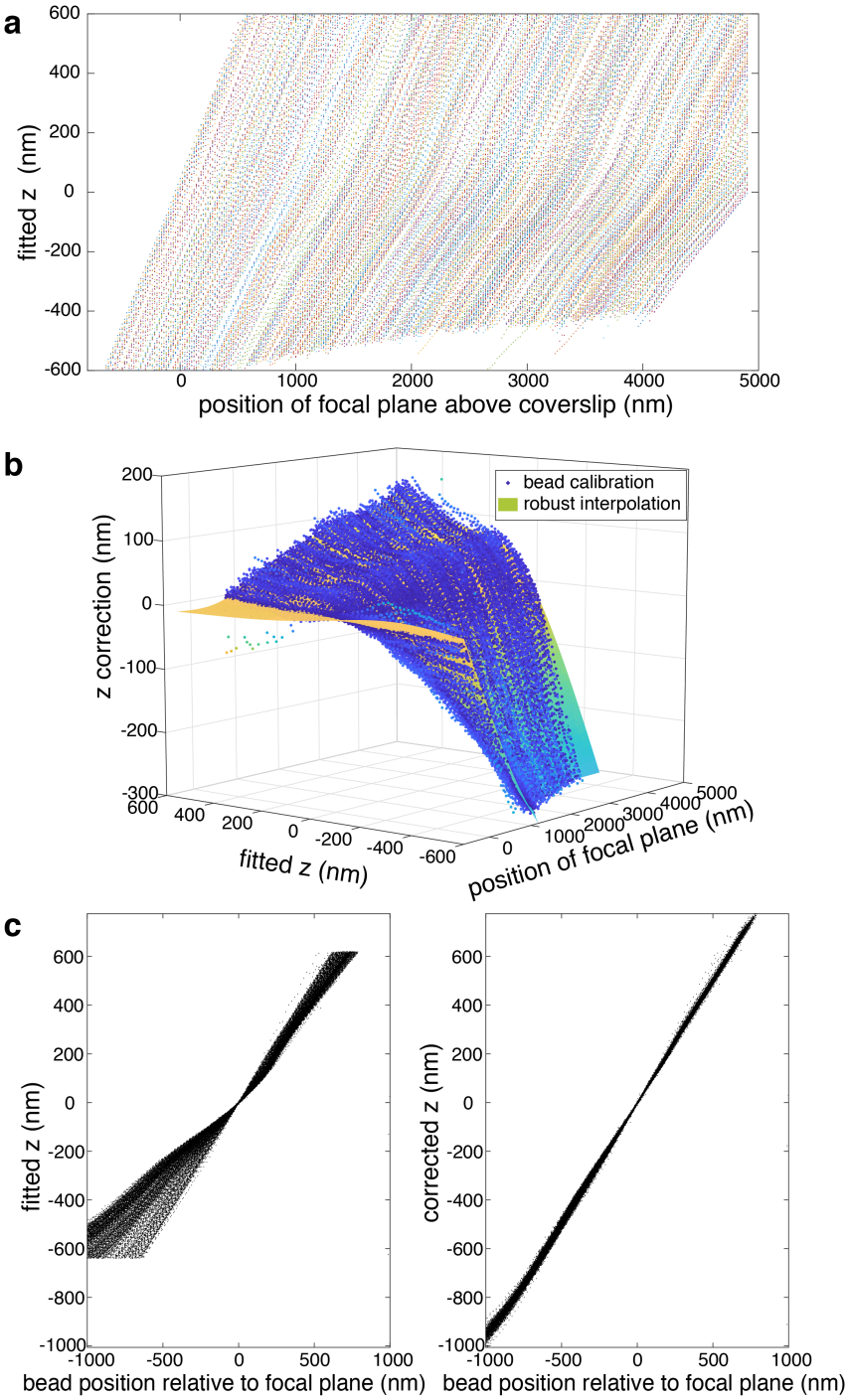

Supplementary Figure 12: Correction of depth-induced aberrations

(**a**) Beads, embedded in an agarose gel, were fitted with a PSF model that was calibrated on the coverslip. For deeper beads, the fitted z-position does not correspond to the distance of the beads from the focal plane. (**b**) Correction for fitted z-values in dependence on the fitted z-values and the position of the focal plane above the coverslip, as described in the **Online Methods**. (**c**) The left panel shows the fitted *z*-positions in dependence on the distance of the bead from the focal plane, and for many beads these are not equal (root mean square (rms) error 148 nm, Pearson correlation coefficient c=0.9848). The right panel shows the corrected *z*-positions, which now show a very high correlation with their distance from the focal plane (rms error 18 nm, Pearson correlation coefficient c=0.9993).

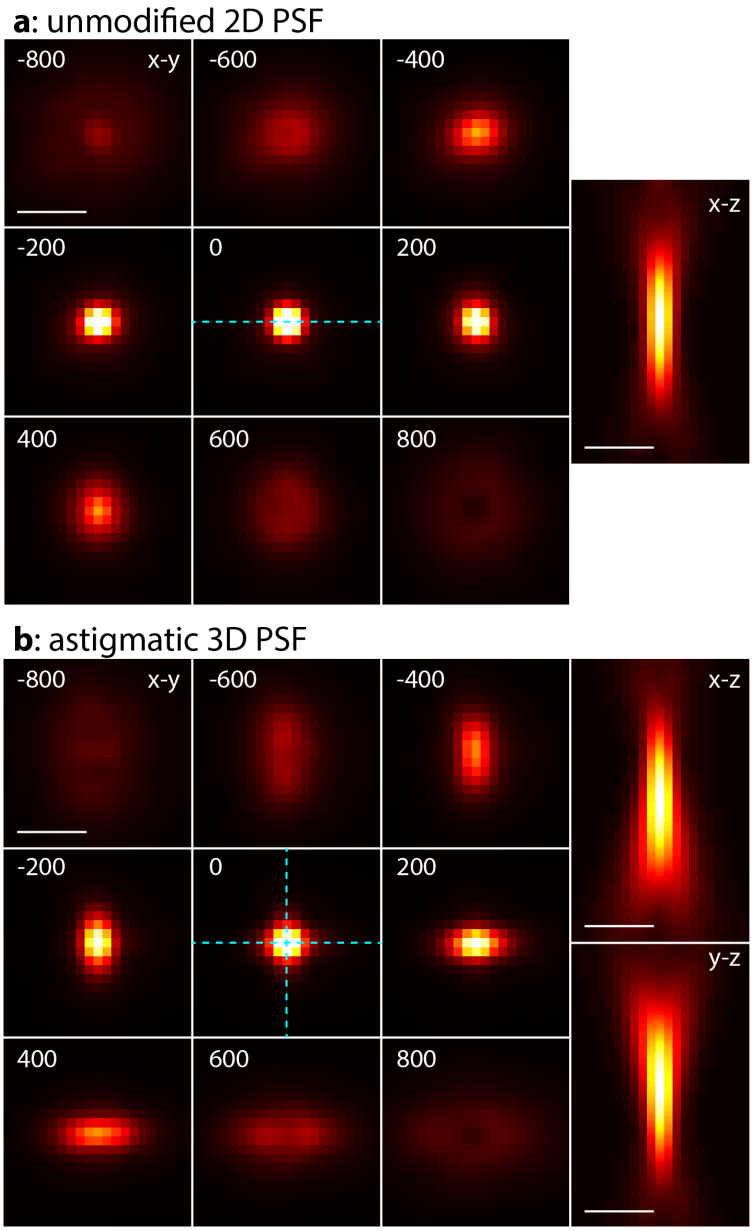

Supplementary Figure 13: Experimental unmodified 2D and astigmatic 3D PSF
(a) The averaged experimental unmodified 2D PSF used in this study. PSFs at axial positions from -800 nm to 800 nm are shown. The *x-z* reconstruction represents a vertical cross-section along the line depicted in the image corresponding to the axial position 0 nm. (**b**) Same as (**a**), but for the averaged experimental astigmatic 3D PSF. Scale bars, 1µm.